Chromosoma (2019) 128:15–20
https://doi.org/10.1007/s00412-018-0684-7

ORIGINAL ARTICLE

Genomic 3D compartments emerge from unfolding mitotic chromosomes

Rajendra Kumar[1,2] · Ludvig Lizana[1,2] · Per Stenberg[3,4]

Received: 14 June 2018 / Revised: 4 October 2018 / Accepted: 7 October 2018 / Published online: 24 October 2018

Abstract

The 3D organisation of the genome in interphase cells is not a randomly folded polymer. Rather, experiments show that chromosomes arrange into a network of 3D compartments that correlate with biological processes, such as transcription, chromatin modifications and protein binding. However, these compartments do not exist during cell division when the DNA is condensed, and it is unclear how and when they emerge. In this paper, we focus on the early stages after cell division as the chromosomes start to decondense. We use a simple polymer model to understand the types of 3D structures that emerge from local unfolding of a compact initial state. From simulations, we recover 3D compartments, such as TADs and A/B compartments that are consistently detected in chromosome capture experiments across cell types and organisms. This suggests that the large-scale 3D organisation is a result of an inflation process.

Keywords Nuclear structure · Polymer simulation · Chromosome decondensation · Hi-C

Introduction

Apart from the bare challenge of packing a long DNA polymer into a small cell nucleus without heavy knotting, the DNA must fold in 3D to allow nuclear processes, such as gene activation, repression and transcription, to run smoothly. By how much the DNA folding patterns influences these processes, and by how much they influence human health, is currently attracting a lot of attention in the scientific community (Cremer and Cremer 2001; Fullwood et al. 2009; Gondor 2013; Krijger and de Laat 2016; Schneider and Grosschedl 2007; Sexton et al. 2007).

To better understand DNA's 3D organisation, researchers developed various chromosome conformation capture methods. The most recent incarnation, the Hi-C method (Lieberman-Aiden et al. 2009), measures contact probabilities between all pairs of loci in the genome. Across cell types and organisms, Hi-C repeatedly detects two types of coexisting megabase-scale structures. First, all chromosome loci seem to belong to one of the two so-called A/B compartments (Lieberman-Aiden et al. 2009), where the chromatin in one compartment is generally more open, accessible and actively transcribed than the other. Second, linear subsections of the genome assemble into topological domains (Dixon et al. 2012; Nora et al. 2012), often referred to as topologically associating domains (TADs), that show up in the Hi-C data as local regions with sharp borders with more internal than external contacts. These borders correlate with several genetic processes, such as transcription, localization of some epigenetic marks and binding positions of several proteins—most notably CTCF and cohesin (Dixon et al. 2012; Nora et al. 2012). However, even though researchers established these correlations, we still lack a general mechanistic understanding for how TADs and A/B compartments form.

To figure out these mechanisms experimentally poses a big challenge. Several research groups have therefore turned to

Electronic supplementary material The online version of this article (https://doi.org/10.1007/s00412-018-0684-7) contains supplementary material, which is available to authorized users.

✉ Ludvig Lizana
ludvig.lizana@umu.se

✉ Per Stenberg
per.stenberg@umu.se

[1] Integrated Science Lab, Umeå University, Umeå, Sweden

[2] Department of Physics, Umeå University, Umeå, Sweden

[3] Department of Ecology and Environmental Science (EMG), Umeå University, Umeå, Sweden

[4] Division of CBRN Security and Defence, FOI-Swedish Defence Research Agency, Umeå, Sweden

computer models (Dekker et al. 2013; Rosa and Zimmer 2014). Apart from the so-called restraint-based models that optimise 3D distances between all DNA fragments using Hi-C data (Fraser et al. 2009), theorists often represent DNA as a polymer fibre (Barbieri et al. 2012; Mirny 2011; Sachs et al. 1995; Therizols et al. 2010). One example is the fractal globule (Grosberg et al. 1993), a compact and knot-free polymer, which is compatible with looping probabilities in the first human Hi-C experiment (Lieberman-Aiden et al. 2009). However, recent work (Sanborn et al. 2015) cast doubt on some of the model's predictions because (1) the looping probability exponent varies on small and large scales (as well as during the cell cycle) and (2) it cannot be used to understand TADs or A/B compartments because fractal globules lack domains. To bridge this gap, researchers developed several mechanistic models. For example, Sanborn et al. (2015) used a ring-like protein (cohesin) that pulls the DNA trough itself until it reaches a CTCF-site where it stops. In another example (Barbieri et al. 2012; Fraser et al. 2015), the authors used a polymer with binding sites to particles that diffused in the surrounding volume. As these particles may simultaneously bind to several sites, they stabilise loops and create nested TADs.

However, while these models can predict TAD-like structures that are formed by loop-stabilising protein complexes, such as CTCF and cohesin, they do not explain A/B compartments. Furthermore, it is unclear if all TADs are loops at all. Moreover, most polymer and restraint-based approaches initially prepare the system in some random configuration and let it equilibrate. With the right set of conditions, the system then folds into domains such as TADs. But, this is far from how the process happens in the cell. Just after cell division, the chromosomes are about 4–50 times more compact on the linear scale (where chromatin which is more open during interphase shows the highest difference) and occupy roughly half the volume than when unfolded during interphase (Belmont 2006; Li et al. 1998; Mora-Bermudez et al. 2007). In addition, mitotic chromosomes seem to lack any clear domain structure (Naumova et al. 2013). This suggests that all domains emerge the chromosome unfolds. This aspect is overlooked in most models. To better understand the types of structural compartments that can emerge from a compact initial state, we used simulations to study the unfolding process of a polymer as subsections decondensed. We find that both TADs and A/B compartments can form without the need to introduce loop-stabilising attractors.

Results and discussion

We model a chromosome as a beads-on-a-string polymer where each bead represents a piece of chromatin. Apart from nearest neighbour harmonic bonds (i.e. Hookean springs), the beads attract each other via a Lennard-Jones potential that also prevents the beads from overlapping. To construct a compact polymer that mimics a mitotic chromosome, we used the GROMACS molecular dynamics package to crumple the polymer into a globule under the Lennard-Jones potential (Fig. 1a). Similar to real Hi-C data on mitotic chromosomes (Naumova et al. 2013), our simulated globule lacks domain structure (see Supporting Fig. S1).

To model the unfolding from the crumpled state, as for example when genes turn on, we partitioned the crumpled polymer into two types of regions that alternate along the polymer (Fig. 1b). Labelled as red and grey, the red parts are more flexible than the grey ones. In our simulations, we achieve this by lowering the Lennard-Jones interaction potential $V(r)$ between red beads (separated by the distance r). In more detail, we lowered the energy scale ε in $V(r) = 4\varepsilon\left[\left(\frac{\sigma}{r}\right)^{12} - \left(\frac{\sigma}{r}\right)^{6}\right]$, to represent a lower "stickiness". For example, compact heterochromatin is considered stickier compared to open chromatin. However, the exact reasons behind this is not completely understood but some studies indicate that histone modifications and HP1 is involved (Antonin and Neumann 2016; Hug et al. 2017; Maison and Almouzni 2004). Finally, the parameter σ is the distance where $V(r = \sigma)$ is zero.

To determine the relative values of ε for different chromatin types, we calculated the radius of gyration as a measure of compactness for polymers where all beads were of the same type (Supporting Fig. S2). During crumpling, we use $\varepsilon = 2.5$ to achieve a condensed globule (Fig. 1a). During the decondensation stage, to reduce computational time when generating a large number of diverse crumpled configurations, we lowered ε to 1.5. This is the highest value of epsilon before the globule starts to unfold (Supporting Fig. S2). This means that ε must be lower than 1.5 for the open-chromatin state. We choose $\varepsilon = 0.75$ for two reasons: (1) If ε is close to 1.5, there will be very little decompaction. (2) If ε is too small, the volume that the unfolded polymer occupies will quickly be very large. In fact, we found that at $\varepsilon = 0.75$, the volume change from the crumpled globule to the decondensed state was roughly twofold (Supporting Fig. S3), which is similar to experimental observations (Mora-Bermudez et al. 2007). However, it should be noted that our simulation does not include a volume barrier, which for real chromosomes would be the nuclear envelope. In Table 1, we summarise the parameter values we used in $V(r)$ during different stages of our simulations.

After crumpling and partitioning, we simulated how the polymer unfolds under thermal fluctuations. Figure 1c shows two snapshots of a simulated polymer. As in all realisations we investigated, these show that the red flexible parts are on the exterior of the polymer, whereas the grey parts remain compact. We stop the simulation after 1,000,000 MD steps where

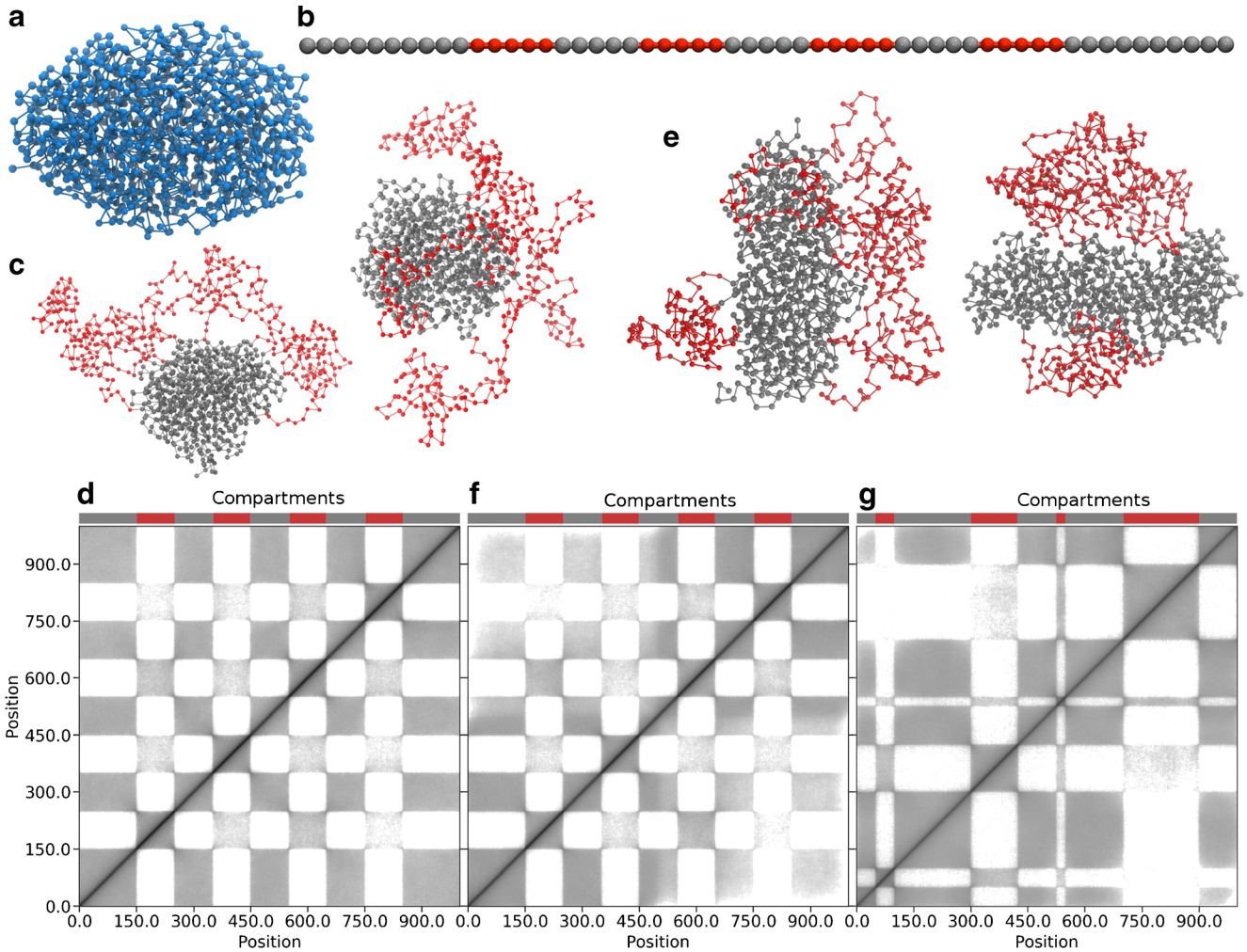

Fig. 1. 3D domains emerge from local unfolding of a compact polymer. **a** An example of a simulated compact polymer. **b** Schematic representation of open (red) and compact (grey) regions (in the simulations we used 1000 beads). **c** Two examples of unfolded polymers starting from a spherical initial condition (no enforced globule elongation). **d** Average bead-bead contact map obtained from an ensemble of polymer structures as those in (**c**). Note the checkerboard pattern. **e** Two unfolded polymers from a cigar-shaped mitotic chromosome-like initial condition (with enforced globule elongation). **f** Average bead-bead contact map obtained from an ensemble of polymer structures as those in (**e**). Note the intensity decay with increasing distance from the diagonal. **g** Contact map where open and compact regions have different lengths

the red parts are clearly decondensed, and then store the structure for analysis. To rapidly generate diverse polymer configurations, we used periodic simulated annealing (see Fig. 2 and details in Supporting Fig. S4).

Table 1 Lennard-Jones parameters used for condensation and decondensation (GROMACS' default unit)

Bead-pair type	σ	ε
Condensation: linear chain to globule		
Bead-bead	0.178	2.5
Decondensation: unfolding of globule		
Close-close	0.178	1.5
Open-open	0.178	0.75
Open-close	0.178	0.05

With the unfolding mechanism in place, we generated an ensemble of unfolded polymers (1000 beads each), all starting from different realisations of the compact globule (Supporting Fig. S4), and then measured the distance between all bead pairs. If the distance between beads' centres was shorter than two times the beads' diameter, we defined it as a physical contact. Collecting all contacts, we made an artificial Hi-C map and normalised it with the KR-norm (Knight and Ruiz 2013), as in real Hi-C experiments. Finally, we visualised the artificial Hi-C map in the gcMapExplorer software (Kumar et al. 2017) (Fig. 1d).

Two things stand out when looking at Fig. 1d: (i) the TAD-like structure along the diagonal and (ii) the off-diagonal plaid pattern that resembles A/B compartments. These two are universal features of all experimental Hi-C maps and also appears here. We get these patterns from a

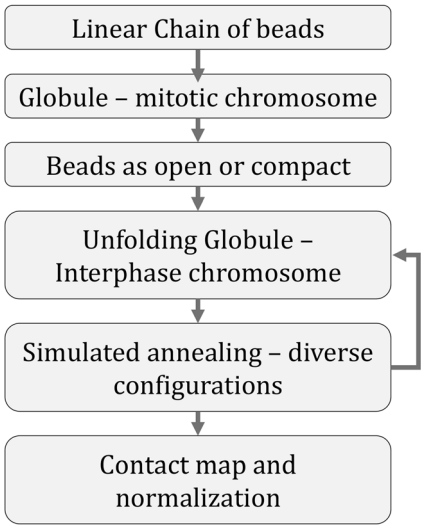

Fig. 2 Summary of the workflow for heterogeneous unfolding of the compact polymer. A more detailed flowchart is provided in Supporting Fig. S1

minimal set of assumptions. In particular, without specific chromatin binding proteins.

However, we observe that the contact frequency in Fig. 1d does not decay as a function of the linear distance between beads (the off-diagonal direction). Apart from short distances, this is not consistent with real Hi-C maps where the intensity decays roughly as a power law with distance (Lieberman-Aiden et al. 2009). The reason is that we used a simple simulation protocol that produces spherically shaped starting configurations (Fig. 1d). To remedy this, we added a global potential (see methods) that gives a cigar-like globule (Fig. 1e). Notably, we do not argue that this is how the mitotic chromosome gets its shape in the cell. It is a pragmatic way to get a starting configuration which is more realistic than a sphere. With this modification to the simulation protocol, we get an intensity that decays with linear distance between bead pairs (Fig. 1f). To further make our system more realistic, we acknowledge that open and compact regions along chromosomes do not have the same length. By varying the length of these in the simulations, the plaid patterns in the contact map (Fig. 1g) approach even more those we observe in real Hi-C maps.

To conclude, we show that partial decondensation of a simple mitotic chromosome-like polymer is enough to recreate TADs, A/B compartments and contact frequency decay over distance—universal features of all (interphase) Hi-C maps across cell types and organisms. Although, our results do not exclude that specific loop-forming proteins are essential to shape and maintain the genomes' 3D structure, our work underscores that chromosomes' large-scale 3D organisation is the result of an inflation process. We look forward to the next-generation 3D genome models that integrate specific interactions, such as loop-stabilising protein complexes and chromatin states, with the initial compact chromosome state.

Methods

We simulated a linear polymer in the GROMACS molecular dynamics package where the beads (or monomers) interact via a Lennard-Jones potential (for convenience we set the bead radius to 1 Å to reduce the problem to atomic scales) $V(r) = 4\varepsilon\left[\left(\frac{\sigma}{r}\right)^{12} - \left(\frac{\sigma}{r}\right)^{6}\right]$. To form a globule, the value of ε was set so that that the resulting attractive force between beads would overcome thermal fluctuations. During decondensation, the value of ε was reduced by 40%, 70% and 98% for interaction between close-close, open-open and close-open beads, respectively. The value of σ was kept constant throughout the simulation (see Table 1).

To condense the polymer into a compact globule, we used GROMACS' Langevin dynamics module. Since creating a large globule (1000 beads) takes time, we made two 500-bead globules and mixed those (Supporting Fig. S4). We then used several cycles of simulated annealing (Supporting Fig. S4) to obtain diverse globule configurations. Furthermore, since the polymers' ends are free, there could be problems with reptation and subsequent knot formation

Table 2 GROMACS MD parameters used during different stages. All parameter values were kept constant, except for the MD steps, which were different depending on the stages

Parameter	Value
Integrator	bd
dt	0.001 ps
Steps	1,000,000,000
Langevin dynamics options	
bd-fric	0
ld-seed	− 1
Neighbour searching parameters	
Cutoff scheme	Group
nstlist	1
rlist	2
Options for van der Waals	
vdw-type	Cutoff
rvdw	2 nm
Temperature coupling	
Tcoupl	v-rescale
nsttcouple	1
tau_t	0.001 ps
ref_t	200 K

(the mitotic chromosome is largely unknotted). To prevent this, the globules' ends were capped by a 10 beads-on-string terminal containing a stiff angular harmonic restraint to prevent bending at the two terminals. To efficiently explore as much of the conformational space as possible, we used a periodic simulated annealing approach detailed in Supporting Fig. S4. The GROMACS parameters we used for the simulations are listed in Table 2.

The above simulation protocol leads to a spherically shaped object. However, the mitotic chromosome is elongated rather than spherical. To achieve this, we used the so-called steered MD simulation with zero pulling velocity. Simply put, we introduced a harmonic pull potential between the centres of masses between the two 500-bead globules while they mixed. After globule formation, we let the globule unfold under thermal fluctuations. In the flexible regions (red beads), we lower the Lennard-Jones parameters compared to the compact region (grey). We show these and all other GROMACS force-field parameters in Table 1 and Table 2.

Funding information This project was funded by the Kempe Foundation (grant number JCK-1347 to LL and PS) and the Knut and Alice Wallenberg Foundation (grant number 2014-0018, to EpiCoN, co-PI: PS). The simulations were performed on resources provided by the Swedish National Infrastructure for Computing (SNIC) at HPC2N Umeå, Sweden.

References

Antonin W, Neumann H (2016) Chromosome condensation and decondensation during mitosis. Curr Opin Cell Biol 40:15–22. https://doi.org/10.1016/j.ceb.2016.01.013

Barbieri M, Chotalia M, Fraser J, Lavitas LM, Dostie J, Pombo A, Nicodemi M (2012) Complexity of chromatin folding is captured by the strings and binders switch model. Proc Natl Acad Sci U S A 109:16173–16178. https://doi.org/10.1073/pnas.1204799109

Belmont AS (2006) Mitotic chromosome structure and condensation. Curr Opin Cell Biol 18:632–638. https://doi.org/10.1016/j.ceb.2006.09.007

Cremer T, Cremer C (2001) Chromosome territories, nuclear architecture and gene regulation in mammalian cells. Nat Rev Genet 2:292–301. https://doi.org/10.1038/35066075

Dekker J, Marti-Renom MA, Mirny LA (2013) Exploring the three-dimensional organization of genomes: interpreting chromatin interaction data. Nat Rev Genet 14:390–403. https://doi.org/10.1038/nrg3454

Dixon JR, Selvaraj S, Yue F, Kim A, Li Y, Shen Y, Hu M, Liu JS, Ren B (2012) Topological domains in mammalian genomes identified by analysis of chromatin interactions. Nature 485:376–380. https://doi.org/10.1038/nature11082

Fraser J, Rousseau M, Shenker S, Ferraiuolo MA, Hayashizaki Y, Blanchette M, Dostie J (2009) Chromatin conformation signatures of cellular differentiation. Genome Biol 10:R37. https://doi.org/10.1186/gb-2009-10-4-r37

Fraser J, Ferrai C, Chiariello AM, Schueler M, Rito T, Laudanno G, Barbieri M, Moore BL, Kraemer DC, Aitken S, Xie SQ, Morris KJ, Itoh M, Kawaji H, Jaeger I, Hayashizaki Y, Carninci P, Forrest AR, The FANTOM Consortium, Semple CA, Dostie J, Pombo A, Nicodemi M (2015) Hierarchical folding and reorganization of chromosomes are linked to transcriptional changes in cellular differentiation. Mol Syst Biol 11:852. https://doi.org/10.15252/msb.20156492

Fullwood MJ, Liu MH, Pan YF, Liu J, Xu H, Mohamed YB, Orlov YL, Velkov S, Ho A, Mei PH, Chew EGY, Huang PYH, Welboren WJ, Han Y, Ooi HS, Ariyaratne PN, Vega VB, Luo Y, Tan PY, Choy PY, Wansa KDSA, Zhao B, Lim KS, Leow SC, Yow JS, Joseph R, Li H, Desai KV, Thomsen JS, Lee YK, Karuturi RKM, Herve T, Bourque G, Stunnenberg HG, Ruan X, Cacheux-Rataboul V, Sung WK, Liu ET, Wei CL, Cheung E, Ruan Y (2009) An oestrogen-receptor-alpha-bound human chromatin interactome. Nature 462:58–64. https://doi.org/10.1038/nature08497

Gondor A (2013) Dynamic chromatin loops bridge health and disease in the nuclear landscape. Semin Cancer Biol 23:90–98. https://doi.org/10.1016/j.semcancer.2013.01.002

Grosberg A, Rabin Y, Havlin S, Neer A (1993) Crumpled globule model of the 3-dimensional structure of DNA. Europhys Lett 23:373–378. https://doi.org/10.1209/0295-5075/23/5/012

Hug CB, Grimaldi AG, Kruse K, Vaquerizas JM (2017) Chromatin architecture emerges during zygotic genome activation independent of transcription. Cell 169:216–228 e219. https://doi.org/10.1016/j.cell.2017.03.024

Knight PA, Ruiz D (2013) A fast algorithm for matrix balancing. IMA J Numer Anal 33:1029–1047. https://doi.org/10.1093/imanum/drs019

Krijger PH, de Laat W (2016) Regulation of disease-associated gene expression in the 3D genome. Nat Rev Mol Cell Biol 17:771–782. https://doi.org/10.1038/nrm.2016.138

Kumar R, Sobhy H, Stenberg P, Lizana L (2017) Genome contact map explorer: a platform for the comparison, interactive visualization and analysis of genome contact maps. Nucleic Acids Res 45:e152. https://doi.org/10.1093/nar/gkx644

Li G, Sudlow G, Belmont AS (1998) Interphase cell cycle dynamics of a late-replicating, heterochromatic homogeneously staining region: precise choreography of condensation/decondensation and nuclear positioning. J Cell Biol 140:975–989

Lieberman-Aiden E, van Berkum NL, Williams L, Imakaev M, Ragoczy T, Telling A, Amit I, Lajoie BR, Sabo PJ, Dorschner MO, Sandstrom R, Bernstein B, Bender MA, Groudine M, Gnirke A, Stamatoyannopoulos J, Mirny LA, Lander ES, Dekker J (2009) Comprehensive mapping of long-range interactions reveals folding principles of the human genome. Science 326:289–293. https://doi.org/10.1126/science.1181369

Maison C, Almouzni G (2004) HP1 and the dynamics of heterochromatin maintenance. Nat Rev Mol Cell Biol 5:296–304. https://doi.org/10.1038/nrm1355

Mirny LA (2011) The fractal globule as a model of chromatin architecture in the cell. Chromosom Res 19:37–51. https://doi.org/10.1007/s10577-010-9177-0

Mora-Bermudez F, Gerlich D, Ellenberg J (2007) Maximal chromosome compaction occurs by axial shortening in anaphase and depends on Aurora kinase. Nat Cell Biol 9:822–831. https://doi.org/10.1038/ncb1606

Naumova N, Imakaev M, Fudenberg G, Zhan Y, Lajoie BR, Mirny LA, Dekker J (2013) Organization of the mitotic chromosome. Science 342:948–953. https://doi.org/10.1126/science.1236083

Nora EP, Lajoie BR, Schulz EG, Giorgetti L, Okamoto I, Servant N, Piolot T, van Berkum NL, Meisig J, Sedat J, Gribnau J, Barillot E, Blüthgen N, Dekker J, Heard E (2012) Spatial partitioning of the regulatory landscape of the X-inactivation centre. Nature 485:381–385. https://doi.org/10.1038/nature11049

Rosa A, Zimmer C (2014) Computational models of large-scale genome architecture. Int Rev Cell Mol Biol 307:275–349. https://doi.org/10.1016/B978-0-12-800046-5.00009-6

Sachs RK, van den Engh G, Trask B, Yokota H, Hearst JE (1995) A random-walk/giant-loop model for interphase chromosomes. Proc Natl Acad Sci U S A 92:2710–2714

Sanborn AL, Rao SSP, Huang SC, Durand NC, Huntley MH, Jewett AI, Bochkov ID, Chinnappan D, Cutkosky A, Li J, Geeting KP, Gnirke A, Melnikov A, McKenna D, Stamenova EK, Lander ES, Aiden EL (2015) Chromatin extrusion explains key features of loop and domain formation in wild-type and engineered genomes. Proc Natl Acad Sci U S A 112:E6456–E6465. https://doi.org/10.1073/pnas.1518552112

Schneider R, Grosschedl R (2007) Dynamics and interplay of nuclear architecture, genome organization, and gene expression. Genes Dev 21:3027–3043. https://doi.org/10.1101/gad.1604607

Sexton T, Schober H, Fraser P, Gasser SM (2007) Gene regulation through nuclear organization. Nat Struct Mol Biol 14:1049–1055. https://doi.org/10.1038/nsmb1324

Therizols P, Duong T, Dujon B, Zimmer C, Fabre E (2010) Chromosome arm length and nuclear constraints determine the dynamic relationship of yeast subtelomeres. Proc Natl Acad Sci U S A 107:2025–2030. https://doi.org/10.1073/pnas.0914187107